

Supplementary Materials (Hep-14-1578)

Liver Fibrosis Occurs Through Dysregulation of MyD88-dependent Innate B cell Activity

Manoj Thapa¹, Raghavan Chinnadurai¹, Victoria Velazquez¹, Dana Tedesco¹, Elizabeth Elrod¹, Jin-Hwan Han¹, Prachi Sharma², Chris Ibegbu¹, Andrew Gewirtz³, Frank Anania⁴, Bali Pulendran⁵, Mehul S. Suthar^{1,6} and Arash Grakoui^{1,7}

¹Emory Vaccine Center, Division of Microbiology and Immunology, Emory University School of Medicine, Atlanta, GA 30322

²Division of Pathology and Laboratory Medicine, Emory University School of Medicine, Atlanta, GA 30322

³Department of Biology, Georgia State University, Atlanta, GA 30303

⁴Division of Digestive Diseases, Emory University School of Medicine, Atlanta, GA 30322

⁵Department of Pathology, Emory University School of Medicine, Atlanta, GA 30322

⁶Department of Pediatrics and Children's Healthcare of Atlanta, Emory University School of Medicine, Atlanta, GA 30322

⁷Division of Infectious diseases, Emory University School of Medicine, Atlanta, Georgia 30322

Keywords: Hepatic stellate cells; retinoic acid; B cells; liver fibrosis, MyD88 signaling.

Contact information

Arash Grakoui, Division of Infectious diseases, Emory Vaccine Center, Division of Microbiology and Immunology, Emory University School of Medicine, Atlanta, GA 30322.

Telephone: +1-404-727-7217; Fax number: +1-404-727-7768; Email:

arash.grakoui@emory.edu

Microarray Analysis for B Cells. B cells (1×10^5) enriched from livers and spleens of oil or CCl_4 -treated mice were resuspended with 350 μl of RLT lysis buffer (Qiagen) mixed with 1% β -mercaptoethanol. RNA was isolated using the RNeasy Micro Kit (Qiagen) according to the manufacturer's protocol. RNA quality was performed on an Agilent 2100 Bioanalyzer (Agilent), and amplification and labeling was performed using the Ovation Pico WTA-system V2 RNA amplification system (NuGen Technologies, Inc.). 5 ng of total RNA was reverse transcribed using a chimeric cDNA/mRNA primer, and a second complementary cDNA strand was synthesized. Purified cDNA was then amplified with ribo-SPIA enzyme and SPIA DNA/RNA primers. Amplified DNA was purified with AMPureXP beads (Beckman Coulter). The concentration of Purified SS-cDNA was measured using the Nanodrop. 5 μg of SS-cDNAs were fragmented and chemically labeled with biotin to generate biotinylated ST-cDNA using Encore biotin module V2. Data were analyzed using Spotfire DecisionSite with OmicsOffice for Microarrays (Integratics Biomarker Discovery). Primary microarray data has been submitted to Gene Expression Omnibus (GEO) in accordance with proposed Minimum Information About a Microarray Experiment (MIAME) standards. A student's t test ($p < 0.001$) was performed to determine the genes that had significantly different expression levels with B cells from CCl_4 -treated compared to levels in B cells from control mice (1.3 fold change). Functional analysis of statistically significant gene expression changes was performed with the MetaCore (Thomson Reuters). For all analyses, a Benjamini-Hochberg test correction was applied to the MetaCore-generated P value to determine the probability that each biological function assigned to that data set was due to chance alone.

Real-time RT-PCR for TLRs. WT splenic B cells (5×10^5) were cultured in presence of retinoic acid (RA, 100nM) with aIgM+aCD40 or aIgM+LPS stimulations. After 48 hrs, RNAs were isolated from cultured B cells using Tri-reagent (Zymo Research, Irvine, CA) and reverse transcribed to cDNA using High Capacity cDNA Reverse Transcription Kits (Applied Biosystem, Grand Island, NY). cDNA was used as a template for quantitative real-time PCR using SYBR Green Master Mix (Applied Biosystem) and the following primers: (all 5'→3') Gapdh F: GTGCCAGCCTCGTCCC, Gapdh R: ACTGTGCCGTTGAATTTGCC; TLR4 F: ACCTGGCTGGTTTACACGTC; TLR4 R: CTGCCAGAGACATTGCAGAA; TLR9 F: ACTGAGCACCCCTGCTTCTA; TLR9 R: AGATTAGTCAGCGGCAGGAA were used. PCR reactions were subjected to 10-min initial hot start at 95°C followed by 40 cycles of amplification 95°C for 10s, 56°C for 35 s, and 72°C for 35 s using a 7500 iCycler (Applied Biosystem). Gene expression was calculated relative to Gapdh.

Supplementary Figure Legends

Supplementary Fig. 1. Serum ALT and α -SMA expression in CCl₄-treated WT mice. (A) WT and mMT mice were treated with either oil or CCl₄ for six wks and mice were processed for isolation of serum and detection of ALT levels. (B) A small segment of liver biopsies were processed for detection of α -SMA (PE) and DAPI (blue) by immunofluorescence staining. (C) Livers were processed for liver non-parenchymal cells (NPCs) isolation as described in Materials and Methods. After density gradient enrichment, NPCs were stained with Abs to CD46 (not shown) and CD45 and analyzed on a FACSAria Cell Sorter II (BD Bioscience) with UV laser. HSCs were identified as UV autofluorescence-positive [UVAF+], CD45-ve and CD146-ve population. For the detection of HSC-associated markers purified liver cells were stained intracellularly with Abs to α -SMA (PE). The expression of α -SMA was analyzed on gated HSC population using FlowJo software (Treestar, Ashland, OR).

Supplementary Fig. 2. HSCs promote survival and plasmablast differentiation (CD138) of hepatic B cells. CD19-enriched hepatic B cells were co-cultured with splenic CD11c⁺ DC or plate-activated HSCs (isolated from livers of WT mice) for 4 d with stimulations as indicated. (A) B cells were stained for Annexin V and 7AAD and (B) percentage (%) of Annexin V⁺ 7AAD⁻ cells shown. (B) B cells were stimulated with anti-IgM as indicated in absence or presence of HSCs and stained for CD138. Data are representative of 2 independent experiments.

Supplementary Fig. 3. HSC-mediated CD138 expression is contact independent. CFSE-labeled splenic B cells were co-cultured with plate-activated HSCs (separated by

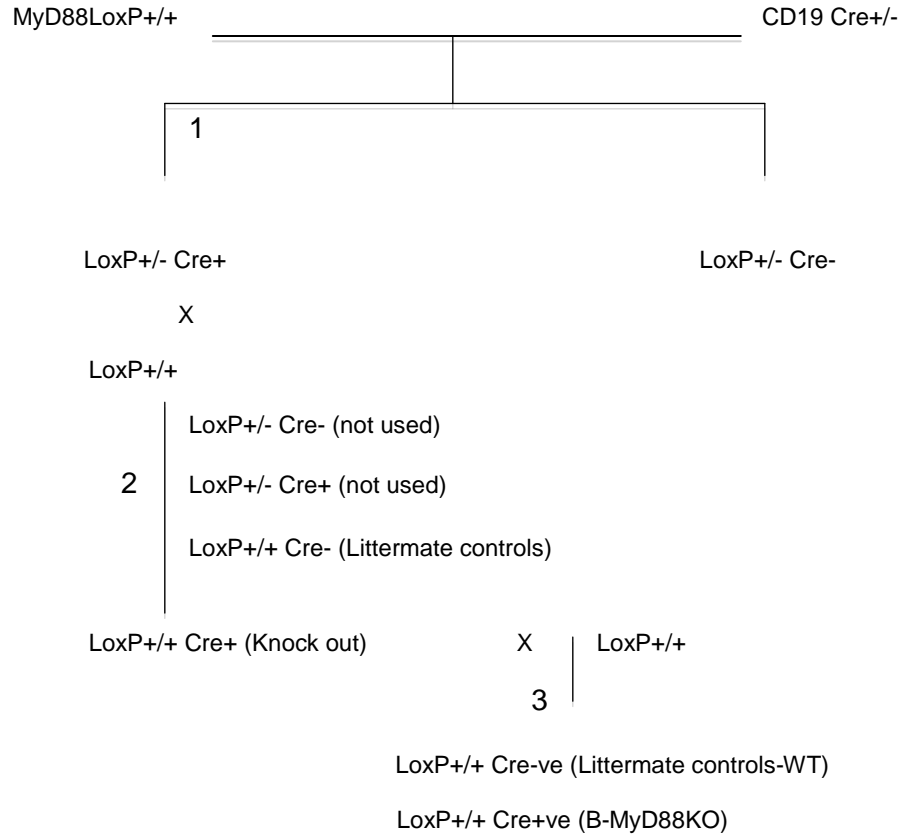
transwell inserts as indicated) for 5 d. (A) After incubation, B cells were stained for CD138 and (B) Culture supernatants were collected and analyzed for IgG production by ELISA. Data are representative of 3 independent experiments.

Supplementary Fig. 4. Retinoic acid enhances TLR4 and TLR9 expressions on B cells. (A) WT splenic B cells (5×10^5) were cultured in presence of retinoic acid (RA) with aIgM+aCD40 or aIgM+LPS stimulation. After 48 hrs, RNAs were isolated from cultured B cells using Tri-reagent and reverse transcribed to cDNA using High Capacity cDNA Reverse Transcription Kits. cDNA was used as a template for quantitative real-time PCR using SYBR Green Master Mix (Applied Biosystem) using murine Gapdh, TLR4 and TLR9 primers as described in Supplementary method section. PCR reactions were subjected to 10min initial hot start at 95°C followed by 40 cycles of amplification 95°C for 10s, 56°C for 35 s, and 72°C for 35 s using a 7500 iCycler (Applied Biosystem). Gene expression was calculated relative to Gapdh. (B) B cells (5×10^5) were cultured for 5 d in presence of retinoic acid (RA) with aIgM+aCD40 or aIgM+LPS stimulation. B cells were processed for TLR4 expression by FACS analysis.

Supplementary Fig. 5. Reduced B cell proliferation and activation in absence of MyD88 signaling. (A) WT and B-MyD88KO mice treated with either oil or CCl₄ for six wk were perfused and livers were removed and processed for B cell isolation. B cells enriched from the livers of WT and B-MyD88KO-CCl₄-treated mice were cultured with stimulation as indicated for 5 d and B cells were processed for staining for KI67 and CD44 by FACS analysis. (B) Mice serum samples were processed for detection of ALT levels. (C) B cells were cultured in presence of LPS for 5 d and supernatants were collected and processed for IgG production by ELISA. Data are representative of two independent

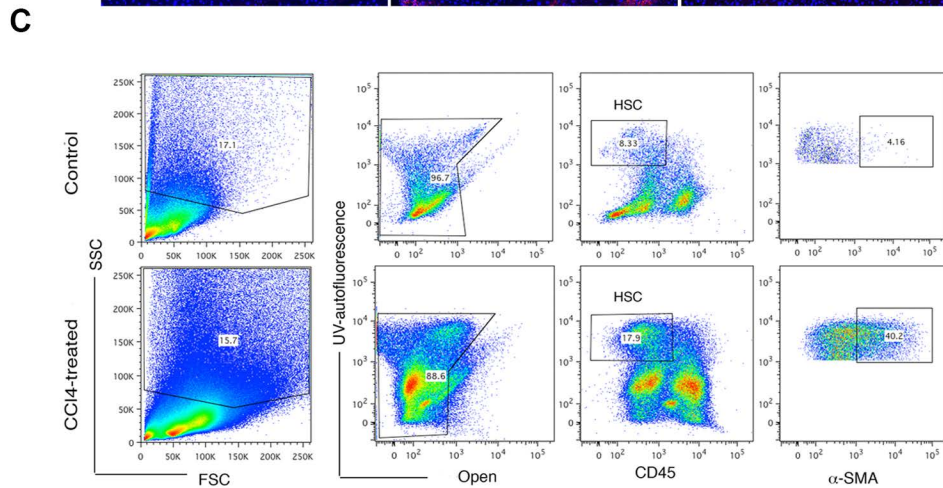
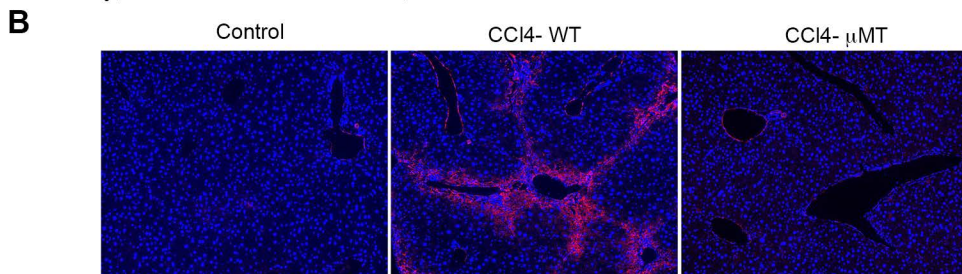
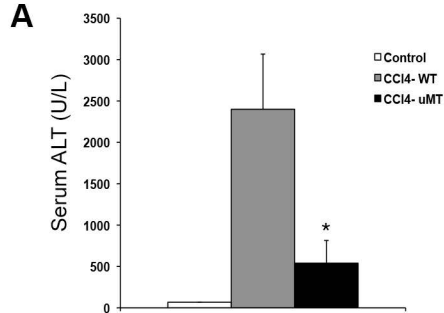
experiments. Two-tailed Student's t test was applied for detection of significance. (* P<.05, ** P<.01).

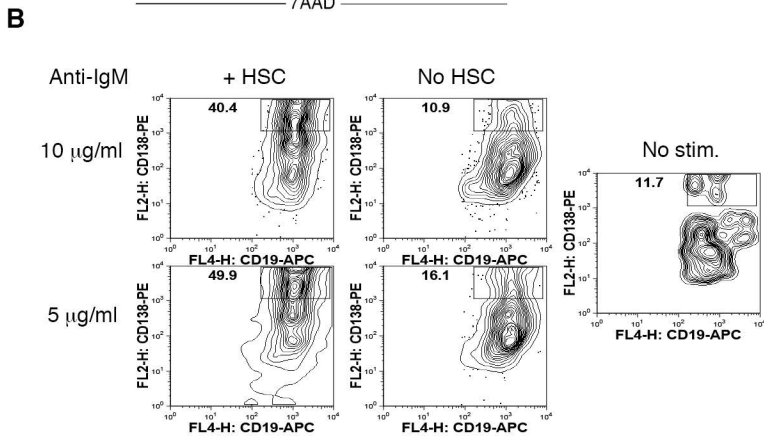
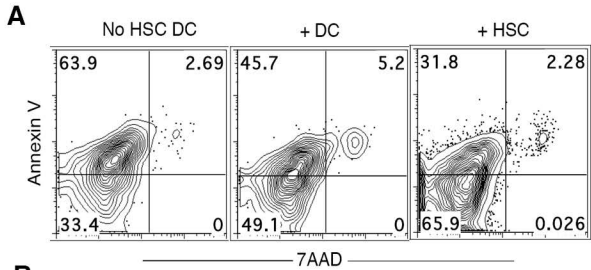
Generation and Confirmation of B-cell-specific MyD88 Deficient Mice (B-MyD88KO)



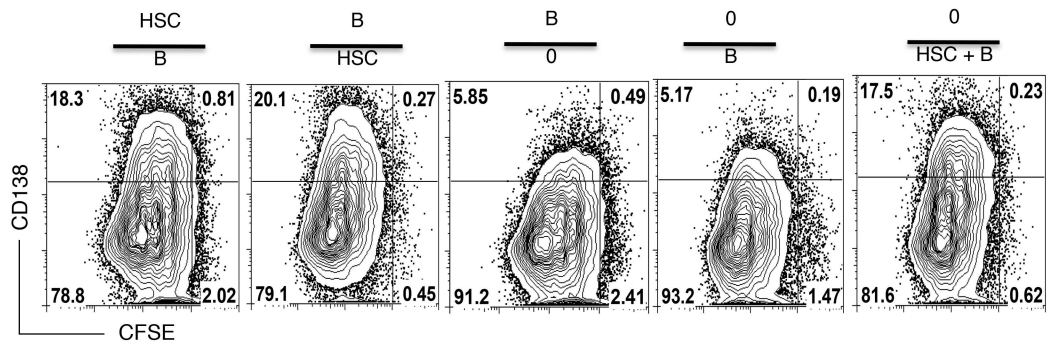
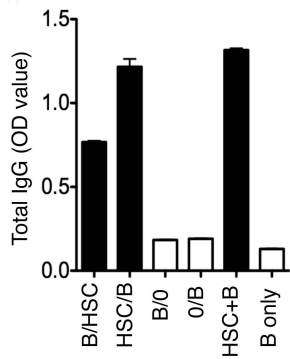
CD19-Cre	Jax#004781	Primers	Interpretation
Primers	CD19-F	AATGTTGTGCTGCCATGCCTC	200 bp (mut)
Specific verified	CD19-R	GTCTGAAGCATTCCACCGGAA	
	CD19-Cre	TTCTTGCGAACCTCATCAC	550 bp (WT)

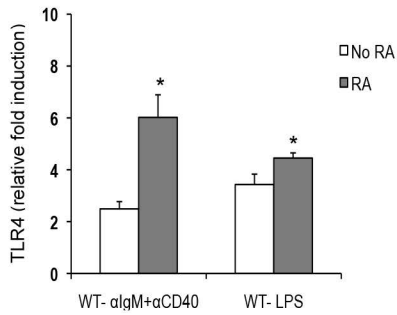
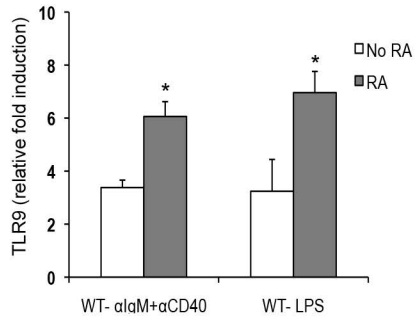
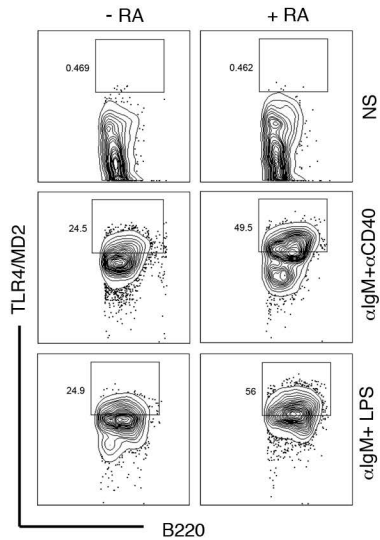
MyD88LoxP (BL/6)	Jax#008888	Primers	Interpretation
Primers	MyD88-LoxP-F	GTTGTGTGTGTCGACCGT	353 bp (mut)
	MYD88-LoxP-R	GTCAGAAACAACCACCATGC	266 bp (WT)



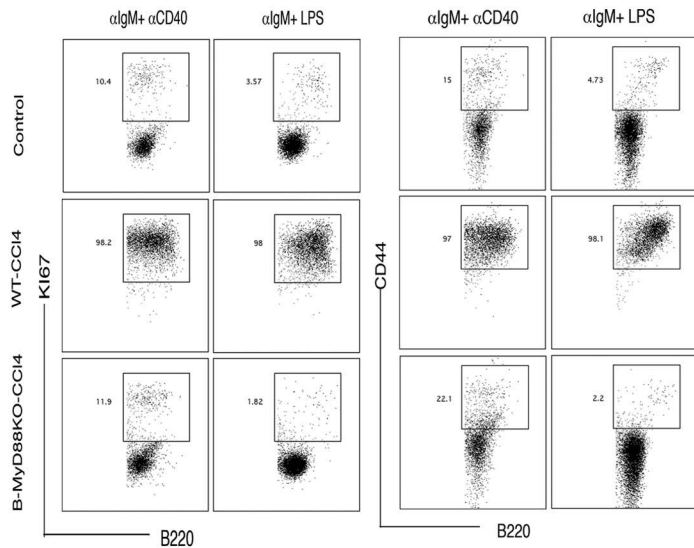
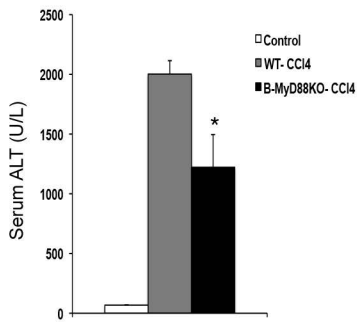
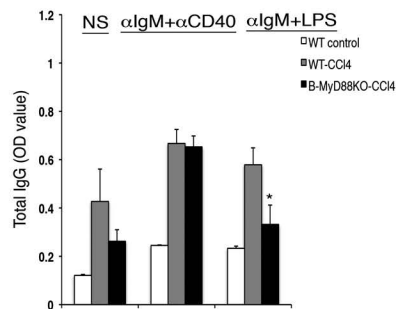


Supplementary Fig. 2.

A**B**

A**B****C**

Supplementary Fig. 4

A**B****C**

Supplementary Fig. 5

HISTOPATHOLOGIC FIBROSIS LESION SCORING

Lesion severity score (hepatocyte necrosis, degeneration, fibrosis, and inflammation)	Score range and description
0	No significant lesion
1	Mild lesion
2	Moderate lesions
3	Severe lesions

HISTOPATHOLOGIC EVALUATION AND FIBROTIC LESION QUANTIFICATION:

No.	Slides	H&E	Masson's Trichrome	Sirius red	Lesion score
1	Control 1	NSL*	NSL	NSL	0
2	Control 2	NSL	NSL	NSL	0
3	Control 3	NSL	NSL	NSL	0
4	CCI4- WT 1	Moderate to severe multifocal hepatocyte necrosis. Mild centrilobular and periportal infiltrates of lymphocytes and few macrophages. Mild hepatocyte, nodular regeneration.	Moderate fibrosis	Moderate fibrosis	3
5	CCI4- WT 2	Severe multifocal hepatocyte necrosis and cytoplasmic vacuolation (degeneration). Moderate to severe centrilobular to periportal infiltration of lymphocytes, neutrophils and macrophages. Moderate multifocal nodular, hepatocyte regeneration.	Severe fibrosis	Severe fibrosis	3
6	CCI4- WT 3	Multifocal, moderate to severe periportal to bridging hepatocyte necrosis and cytoplasmic vacuolation (degeneration). Moderate, occasional, centrilobular to periportal infiltration of lymphocytes, neutrophils and macrophages.	Severe fibrosis	Severe fibrosis	3
7	CCI4- mMT 1	NSL	Mild fibrosis	Mild fibrosis	1
8	CCI4- mMT 2	Multifocal, moderate nodular, hepatocyte regeneration, focal dilation of hepatic sinusoids.	Mild fibrosis	Mild fibrosis	1
9	CCI4- mMT 3	NSL	No fibrosis	No fibrosis	0

*NSL=No significant lesion